Am J Transl Res 2025;17(11):8896-8906
www.ajtr.org /ISSN:1943-8141/AJTR0161407

Original Article

TNXB modulates radiosensitivity of esophageal cancer through the ATM/P53 pathway

Huiying Yang[1], Ning Xu[1], Xiaoling Cao[1], Xiaoteng Wang[2], Linlin Sun[1], Weiwei Jiang[1], Shaojiao Mu[1], Qiankun Li[1], Wenjing Yue[1], Jian Gan[1], Ming Li[1], Wenjian Zhang[3], Yipin Liu[1]

[1]Department of Gastroenterology, Binzhou Medical College Yantai Affiliated Hospital, Yantai 264100, Shandong, China; [2]Binzhou Medical College Yantai Campus, Yantai 264000, Shandong, China; [3]Department of Thoracic Surgery, Weihai Municipal Hospital, Weihai 264299, Shandong, China

Received October 23, 2024; Accepted February 7, 2025; Epub November 15, 2025; Published November 30, 2025

Abstract: Objective: Esophageal carcinoma (ESCA) is a common malignancy, and modulating radiosensitivity is crucial for individualized treatment. Tenascin XB (TNXB) overexpression in tumors is speculated to influence radiosensitivity. This study aims to investigate whether TNXB overexpression prior to irradiation sensitizes human ESCA cells *in vitro*. Methods: The expression of TNXB in tumor specimens was examined using Real-time quantitative polymerase chain reaction (RT-qPCR) and immunohistochemistry. The relationships between TNXB expression and clinicopathological characteristics were analyzed. Two human ESCA cell lines (TE-1 and OE33) were subjected to explore the effect of TNXB expression on radiosensitivity. DNA damage, apoptosis, cell cycle arrest, and protein expression were assessed by colony formation assay, western blotting and flow cytometry, respectively. Results: TNXB displayed a low expression in tumor tissues. Reduced TNXB expression was significantly correlated with larger tumor size and higher TNM stage. TNXB overexpression coupled with X-ray irradiation markedly suppressed colony formation in TE-1 and OE33 cells, and increased γH2AX expression, apoptosis rate, and promoted cell cycle arrest. Additionally, the combined treatment of TNXB overexpression and X-ray irradiation resulted in upregulation and phosphorylation of Ataxia Telangiectasia Mutated (ATM) and P53, leading to elevated cleaved-caspase3 and decreased pro-caspase3 levels. si-ATM treatment reversed these effects. Conclusion: Our findings demonstrate that TNXB enhances radiosensitivity in TE-1 and TE-10 cells by the ATM/P53 pathway.

Keywords: TNXB, esophageal squamous cell carcinoma, radiosensitivity, ATM, P53

Introduction

Esophageal carcinoma (ESCA) remains one of the most aggressive malignancies worldwide with a poor prognosis and a 5-year overall survival (OS) rate of less than 20% [1, 2]. Radiotherapy has emerged as a mainstay curative treatment for locally advanced ESCA [3, 4]. Approximately 38.7% of stage II ESCA patients and 20% of stage III ESCA patients are highly sensitive to radiotherapy, contributing to pathologic complete response [3, 5, 6]. However, some patients do not benefit from radiotherapy in terms of survival or quality of life, since their ESCA is intrinsically resistant to radiation [7]. Therefore, identifying molecular targets and pathways that mediate radiosensitivity is crucial for the development of individualized treatment for ESCA.

Tenascin-X (TNX), composed of TNXA and TNXB, is a member (450 kDa) of the tenascin family of extracellular matrix (ECM) glycoproteins. Its deficiency is linked to various disorders affecting collagen organization and matrix integrity, particularly in joints, skin, and vessels [8, 9]. TNXB has been reported to be abnormally expressed in several cancers, including ovarian carcinoma [10], medullary thyroid carcinoma [11], and gastric cancer [12]. Additionally, elevated TNXB level is associated with an increased risk of breast cancer [13]. Nan et al. reported that TNXB expression is low in ESCA, and both knockdown and knockout of TNXB significantly accelerated cell growth *in vitro* [14]. However, the role and mechanisms of TNXB in the radiosensitivity of ESCA remain poorly understood.

https://doi.org/10.62347/AAC03727

In the present study, we used a plasmid-mediated TNXB overexpression strategy to investigate the effect and underlying mechanism of combined irradiation and TNXB overexpression on cell growth, apoptosis, and cell cycle arrest. Our findings may provide valuable insight into the development of individualized treatments for ESCA.

Materials and methods

Tissue samples

All patients selected for this study were diagnosed with ESCA, and tumors were classified according to the Union International Contre le Cancer (UICC) Guidelines for esophagal cancer. After obtaining the informed consent from all participants, 60 esophageal cancer tissue specimens and 34 non-cancerous adjacent tissue specimens were collected. This study was approved by the Ethics Committee of Weihai Municipal Hospital (20230124).

Immunohistochemistry

Consecutive 4 μm thick sections were cut and examined by immunohistochemistry. Each specimen was deparaffinized in xylene and dehydrated through gradient ethanol/water. Antigen retrieval was performed by heating the slides in 0.01 M citrate buffer (pH 6.0) in a microwave oven for 10 minutes. The slides were blocked with BSA solution for 20 minutes at room temperature to prevent non-specific binding. Sections were incubated at 37°C for 60 minutes with primary anti-TNXB antibodies (1:200 dilution), followed by rinsing with phosphate-buffer saline (PBS) for 3 times. Sections were subsequently incubated with goat anti-rabbit IgG antibody for 30 min and rinsed with PBS for 10 min. The signal was visualized by incubating the slides in SABC kit (Beyotime, Shanghai, China) for approximately 20 min at 37°C, then stained with DAB color kit (Beyotime, Shanghai, China). Subsequently, the sections were counterstained with hematoxylin and dehydrated using a graded series of alcohols. The frequency of TNXB-positive cells was scored according to the percentage of positive cells: 0% was deemed negative, 1-25% was (+/1), 26-50% was (++/2) and > 51% was (+++/3). The intensity of TNXB expression was scored based on the following standard: weak = 1, moderate = 2, and strong = 3. The average TNXB expression of each section = intensity × percent frequency. A score ≤ 2 was considered low expression, and a score > 2 was high expression.

RT-qPCR

Total RNA was extracted from tissue samples using the RNeasy Mini Kit (Qiagen, Valencia, CA, USA), and cDNA was synthesized from 1 μg of total RNA using the First Strand cDNA Synthesis Kit (Invitrogen, Carlsbad, CA, USA) according to the manufacturer's instructions. RT-PCR was carried out using the SYBR Green PCR Core Reagents Kit (Thermo Fisher Scientific, MA, USA). The $2^{-\Delta\Delta Ct}$ method was conducted to determine the fold changes in gene expression levels among specimens. Beta-actin-specific PCR products served as an internal control. The primers were designed and synthesized by GenePharma (Shanghai, China). The primer sequences were: TNXB: 5'-GTGGTCCAGTATGAGGACACG-3'; 5'-CTGGTGGTCACGTCAGTCAC-3'; β-actin: 5'-ATTGGCAATGAGCGGTTC-3'; 5'-CGTGGATGCCACAGGACT-3'.

Cell lines

Four ESCA cell lines (KYSE-510, OE33, TE-10 and TE-1) and normal esophageal epithelial HEEC cells were purchased from TongPai Technology (Shanghai, China). All cell lines were maintained in RPMI-1640 (Gibco, Thermo Fisher Scientific, MA, USA) containing 10% fetal bovine serum and 1% penicillin-streptomycin (Gibco, Thermo Fisher Scientific, MA, USA) at 37°C in a 5% CO_2 incubator.

Cell transfection

The TNXB-overexpression vector (pcDNA3-FLAG TNXB), control vector pcDNA3, and ataxia-telangiectasia mutated (ATM) knockdown plasmid were synthesized by GenePharma (Shanghai, China). ESCA cell lines were transiently transfected with these vectors (2.5 mg/well in 6-well plates) using Lipofectamine® 2000 (Thermo Fisher Scientific, MA, USA) according to the manufacturer's instructions. After 24 h, the culture medium was replaced, and the cells were used for subsequent experiments.

γ-irradiation

The cells were divided into different groups and irradiated with (0 or 4 Gy) γ-rays using Siemens Primus accelerators. Following irradiation, cells were collected for subsequent experiments.

Western blotting

Cells were digested with trypsin, harvested after transfection or ray irradiation, and then lysed in 0.5 mL RIPA lysis buffer (Beyotime, Shanghai, China). The lysates were centrifuged at 4°C, 12000 r/min for 5 min. The protein concentration was qualified with a BCA kit (Beyotime, Shanghai, China). Total proteins were separated by 10% SDS-PAGE and electrotransferred to a polyvinylidene fluoride membrane (Roche, Germany). The membranes were blocked with TBST containing 0.1% Tween-20 and 5% non-fat dried milk for 1 h at room temperature. The membranes were incubated overnight at 4°C with polyclonal primary antibody: anti-human TNXB (1:2000, Thermo Fisher Scientific, MA, USA), Cleaved-Caspase 3 Rabbit mAb (1:1000, cat. no. 9664), Caspase-3 Mouse mAb (1:1000, cat. no. 9668), β-actin Rabbit mAb (1:1000, cat. no. 8457), ATM Rabbit mAb (1:1000, cat. no. 2873), p-ATM Rabbit mAb (1:1000, cat. no. 13050), p53 Rabbit mAb (1:1000, cat. no. 2527), p-p53 Rabbit mAb (1:1000, cat. no. 82530), and γH2AX Rabbit mAb (1:1000, cat. no. 9718, all Cell Signaling Technology, Shanghai, China). The membranes were washed with TBST thrice and incubated with HRP-conjugated goat anti-mouse or goat anti-rabbit IgG (1:1000, cat. no. 7076 or 7074) for 1 h at room temperature. Immunoreactive signals were detected using a chemiluminescence kit (Amersham Biosciences).

Clonogenic assay

TE-1 and OE33 cells were irradiated with 4 Gy after transfection, then harvested and seeded into 6-well plates with serum-containing media. The cells were allowed to grow for 10 days until visible colonies appeared. The colonies were then washed with PBS, fixed with 4% paraformaldehyde and stained with 0.1% crystal violet for 15 minutes. Only colonies with more than 50 cells were counted to confirm cell proliferation activity.

Flow cytometry

Cell apoptosis was assessed using the FITC Annexin V Apoptosis Detection Kit (Beyotime, Shanghai, China) according to the manufacturer's instructions. After transfection combined with 4 Gy radiation, cells were stained with 5 μL of FITC Annexin V and 5 μL of PI for 20 minutes in darkness at room temperature. For cell cycle analysis, cells were irradiated with 4 Gy after transfection, then harvested and fixed with 70% chilled ethanol overnight. The cells were labeled with PI (Beyotime) for 30 minutes in the dark at 37°C. Apoptosis and cell cycle phases were analyzed using a BD Accuri C6 flow cytometer.

Statistical analysis

All data were expressed as mean ± SD and analyzed using SPSS 25.0 (IBM Corporation, Chicago, IL, USA). The chi-square test was performed to estimate the correlation between TNXB expression and clinicopathologic characteristics. A t-test was used for comparisons between two groups, while comparisons among multiple groups were performed using ANOVA followed by the Tukey test. A P-value < 0.05 was considered significant.

Results

Expression of TNXB in ESCA tissues

We first examined the expression of TNXB in ESCA tissues (T) and corresponding nonneoplastic tissues (N) using the GEPIA database (http://gepia.cancer-pku.cn). The results showed that TNXB expression was dramatically downregulated in ESCA tissues compared to normal tissues (**Figure 1A**). Next, we evaluated the expression of TNXB in ESCA tissues and adjacent normal tissues using RT-qPCR. The TNXB mRNA level in ESCA tissues was lower than that of the non-tumorous tissues (**Figure 1B**). To confirm the low expression of TNXB in ESCA tissues, Immunohistochemistry was performed on ESCA tissue specimens with normal adjacent tissue as a positive control. TNXB was primarily expressed in the cytoplasm of ESCA cells. These results were consistent with the RT-qPCR results (**Figure 1C**). Of the total 60 cases, 48 cases were classified as having low TNXB expression, and 12 cases had non-low expression. All adjacent tissues exhibited positive or high TNXB expression. The correlations between TNXB expression levels and factors such as ages, gender, tumor sizes, clinical stage, and lymph nodes metastasis were analyzed (**Table 1**). Low TNXB expression was significantly associated with larger tumor size ($P = 0.0089$) and higher TNM stage ($P = 0.004$). However, no significant correlation was found between TNXB expression and gender, age, T status, or lymph node metastasis ($P > 0.05$).

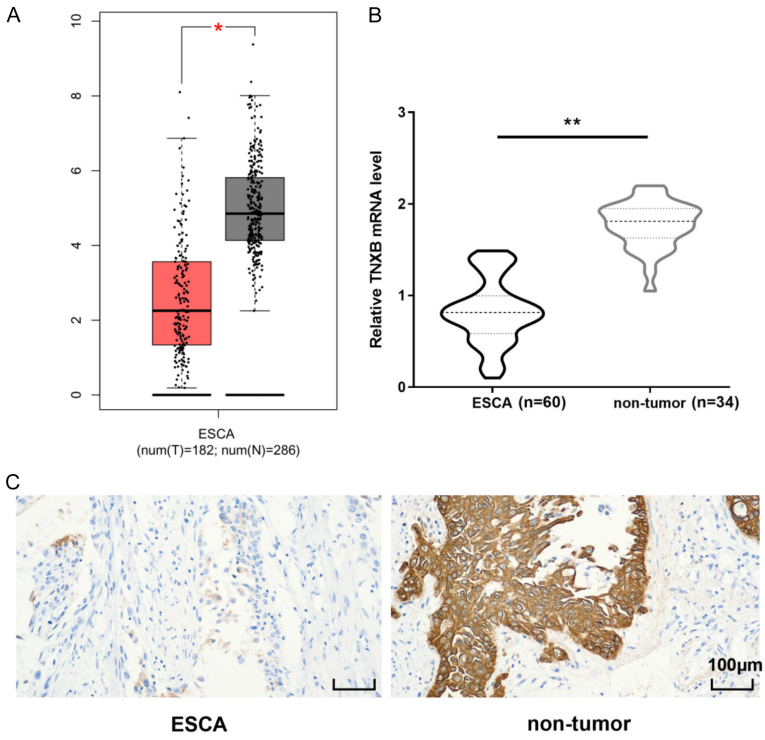

Figure 1. TNXB was downregulated in ESCA. A. The expression of TNXB in ESCA tissue (T) and corresponding nonneoplastic tissue (N) were examined using the GEPIA database. B. The expression of TNXB in ESCA tissues and adjacent normal tissues was detected using RT-qPCR. C. Expression of TNXB in ESCA tissues and adjacent normal tissues observed using immunohistochemistry. **P < 0.01. TNXB: Tenascin XB; ESCA: esophageal carcinoma; RT-qPCR: real-time quantitative polymerase chain reaction; GEPIA: Gene Expression Profiling Interactive Analysis.

TNXB overexpression enhanced the radiosensitivity of ESCA cell lines

To investigate the biological function of TNXB in radiotherapy sensitivity, we detected its expression in four ESCA cell lines and selected those with low TNXB expression for subsequent loss-of-function experiments. Compared to HEEC cells, TNXB expression was notably low in four ESCA cell lines (KYSE-510, OE33, TE-10, and TE-1), with TE-1 and OE33 cell lines showing the most significant decrease (**Figure 2A**). We then used a pcDNA3 vector-mediated system to induce TNXB overexpression in TE-1 and OE33 cell lines (TE-1-Oe-TNXB 1# and TE-1-Oe-TNXB 2#) or (OE33-Oe-TNXB 1# and OE33-Oe-TNXB 2#). Cells transfected with Oe-TNXB 1# exhibited the highest TNXB expression (**Figure 2B**), and these cells were designated as OeTNXB cells for further experiments. Colony formation assays were applied to investigate the correlation between TNXB expression and radiosensitivity in TE-1 and OE33 cells. The results showed that TNXB overexpression markedly increased cell apoptosis in TE-1 and OE33 cells compared to NC groups. Furthermore, in the combination of Oe-TNXB and 4 Gy groups, TE-1 and OE33 cells exhibited a lower survival rate compared to the 4 Gy-only group (**Figure 2C**).

To explore the mechanisms underlying TNXB-induced radiosensitivity, we assessed the expression of phosphorylated histone H2AX (γ-H2AX), a marker of DNA damage, through western blotting. After irradiation, the expression of γ-H2AX was significantly higher in TE-1-Oe-TNXB and OE33-Oe-TNXB cells than in the irradiation alone group (**Figure 2D**). Since apoptosis is a pivotal cellular response to radiotherapy, we further confirmed the apoptosis rates by flow cytometry. TNXB overexpression markedly enhanced cell apoptosis in TE-1 and OE33 cells compared to NC groups, indicating that TNXB overexpression enhanced radiation-induced apoptosis. The apoptosis rates in the Oe-TNXB combined with 4 Gy group were significantly higher than in the 4 Gy group (**Figure 3A**). Subsequently, cell cycle results showed that TNXB overexpression led to an increase in the G2/M cell population in TE-1 and OE33 cells. The G2/M proportion in the Oe-TNXB combined with 4 Gy group was significantly higher than that of the 4 Gy-alone group (**Figure 3B**). These findings suggest that TNXB overexpression enhances radiotherapy-induced DNA damage, apoptosis, and G2/M arrest.

TNXB enhanced the radiosensitivity through the ATM/P53 pathway

To investigate the mechanism through which TNXB influences radiosensitivity, we performed western blot analysis to evaluate the key elements of the DNA damage response network, including ATM, p53, their phosphorylated forms, and downstream apoptotic proteins (**Figure**

Table 1. Correlations of TNXB expression with clinicopathologic characteristics in ESCA patients

Data	Case	TNXB		*P* value
		Low expression (n = 35)	Overexpression (n = 25)	
Age (years)				0.822
≥ 50	37	22	15	
< 50	23	13	10	
Gender				0.930
Female	34	20	14	
Male	26	15	11	
Tumor size (cm)				0.008
≥ 3	24	9	15	
< 3	36	26	10	
T status				0.066
T1-2	23	10	13	
T3-4	37	25	12	
Lymph node status				0.564
N0	19	9	11	
N1-2	31	16	14	
TNM stage				0.004
I + II	21	7	14	
III + IV	39	28	11	

4A). The results showed that TNXB overexpression markedly increased the expression of ATM, P53, p-ATM and p-P53 in TE-1 and OE33 cells compared to NC groups. In TE-1 cells, the combination of Oe-TNXB and 4 Gy treatment resulted in higher levels of ATM, P53, p-ATM and p-P53 compared to the 4 Gy-only group. Moreover, irradiation increased the expression of cleaved-caspase-3, while the expression of procaspase-3 was reduced in TE-1 cells. TNXB overexpression also decreased the expression of pro-caspase-3 and enhanced the expression of cleaved-caspase-3, further confirming that TNXB regulates radiosensitivity by the ATM/p53 pathway and its downstream apoptotic proteins in ESCA cells.

To further verify this conjecture, we constructed ATM knockdown cell lines using the si-ATM vectors (#1 and #2). si-ATM vector transfection resulted in decreased ATM expression in TE-1 and OE33 cells, with vector #1 showing the most significant reduction, which was selected for subsequent experiments (**Figure 4B**). Colony formation assays revealed that si-ATM significantly attenuated the TNXB overexpression-induced decrease in cell proliferation in TE-1 and OE33 cells compared to the 4 Gy + Oe-TNXB group (**Figure 4C**). Western blot assay showed that the si-ATM significantly reduced the TNXB overexpression induced - increase in γ-H2AX expression in both groups (**Figure 4D**). Flow cytometry assay revealed that si-ATM reversed the TNXB overexpression-induced apoptosis (**Figure 5A**) and G2/M arrest (**Figure 5B**) in TE-1 and OE33 cells compared to the Oe-TNXB combined with 4 Gy group. Additionally, si-ATM significantly inhibited the TNXB overexpression-induced increase in P53, p-P53, and cleaved-caspase-3, and the decrease in pro-caspase-3 levels in TE-1 and OE33 cells compared to the 4 Gy + Oe-TNXB group (**Figure 5C**). These findings suggest that TNXB enhances radiotherapy-induced DNA damage, apoptosis, and G2/M arrest by activating the ATM/p53 pathway.

Discussion

Due to the inherent insensitivity of ESCA to radiotherapy, patients often experience local recurrence and poor survival rates [15]. Therefore, identifying new molecular targets and pathways that mediate radiosensitivity is crucial for the individualized treatment of ESCA.

TNXB plays a key role in maintaining collagen organization and matrix integrity [14], and its expression is gradually reduced during the tumorigenesis of gastric cancer [12], yet restored in malignant mesotheliomas [16]. While the

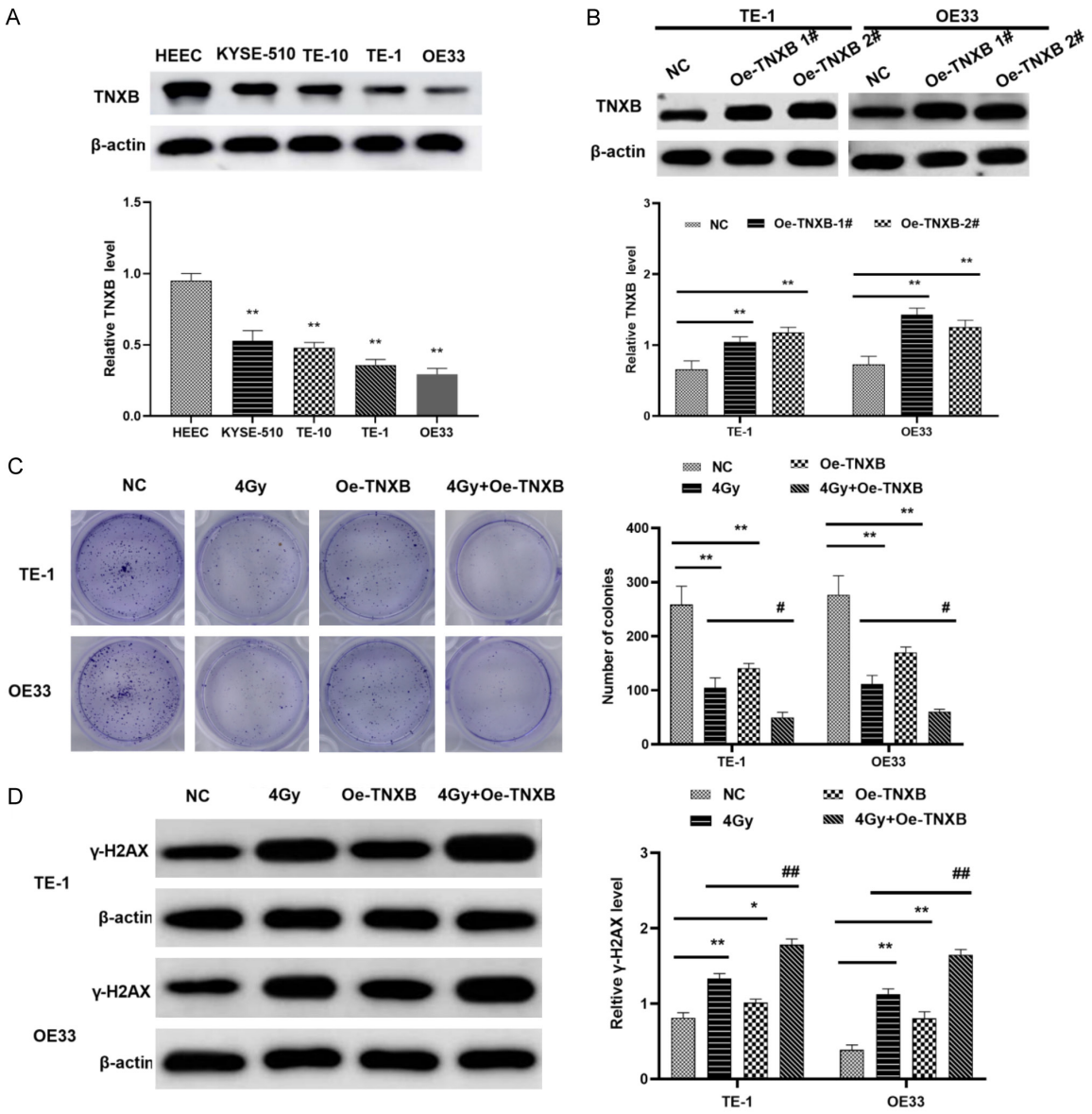

Figure 2. TNXB overexpression enhanced radiotherapy-induced DNA damage in ESCA cell lines. A. Expression of TNXB in HEEC and four ESCA cell lines (KYSE-510, OE33, TE-10, and TE-1). B. Transfection efficiency of Oe-TNXB 1# and Oe-TNXB 2# in TE-1 and OE33 cell lines. C. Effects of TNXB overexpression, 4 Gy radiation and their combination on colony formation of TE-1 and OE33 cells. D. Expression of γ-H2AX in TE-1-Oe-TNXB and OE33-Oe-TNXB cells using western blot assay. *P < 0.05, **P < 0.01; #P < 0.05, ##P < 0.01.

aberrant expression of TNXB has been implicated in the prognosis of various cancers, its role in ESCA remains unclear. In the current study, we discovered that TNXB expression was strikingly downregulated in ESCA tissues compared to adjacent noncancerous tissues. Moreover, stage III-IV ESCA patients often exhibited notably lower TNXB expression. These findings align with previous research by Nan et al. [14].

While TNXB expression has been associated with poor prognosis, its effect on radiosensitivity has remained unclear [17, 18]. Our *in vitro* phenotypic experiments confirmed that TNXB influences radiosensitivity: irradiation resulted in a lower colony formation rate, increased γH2AX expression, enhanced apoptosis, and greater cell cycle arrest [19-21]. Moreover, TNXB overexpression was linked to increased expression and phosphorylation of ATM and p53.

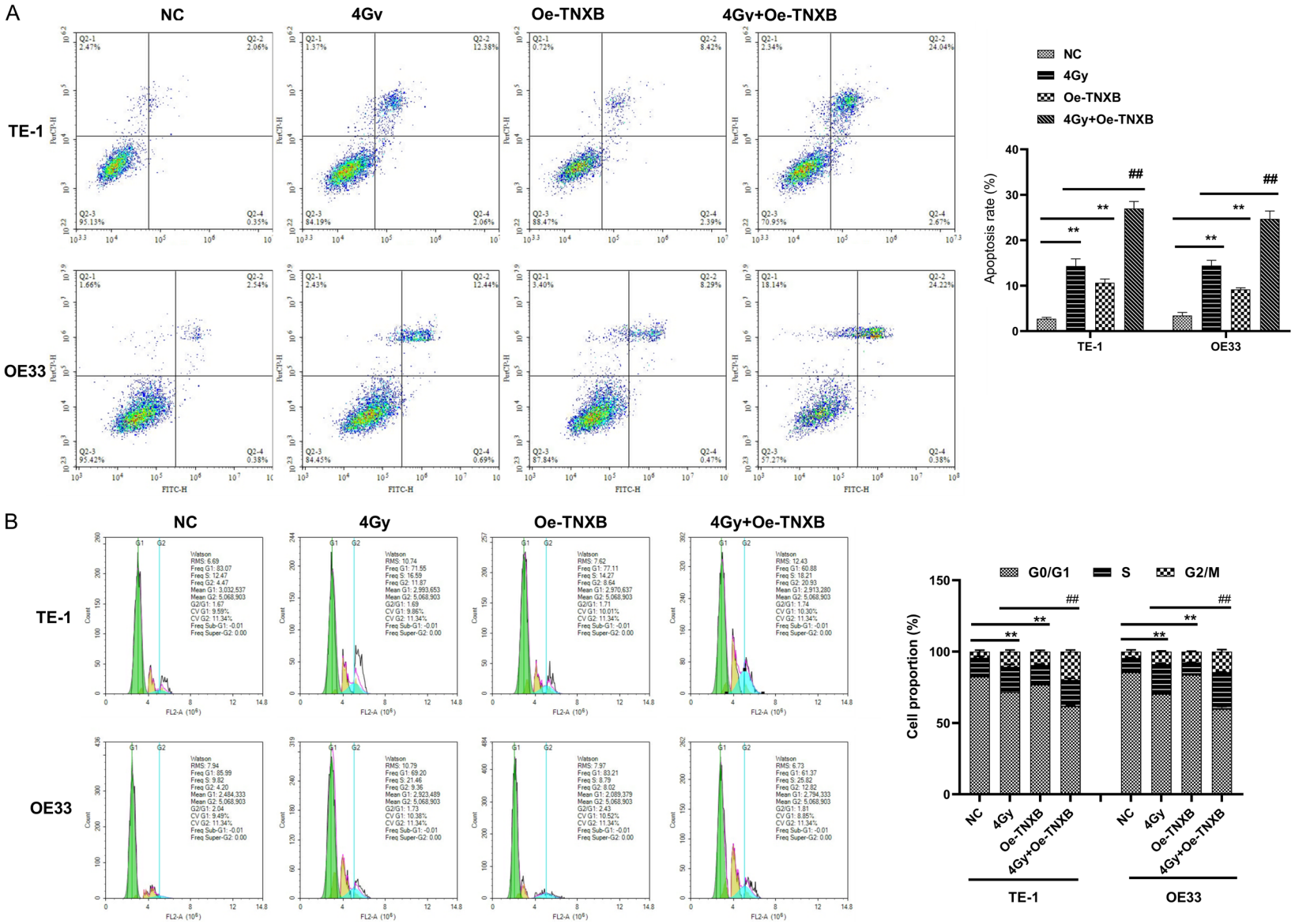

Figure 3. TNXB overexpression enhanced radiotherapy-induced apoptosis and G2/M arrest in ESCA cell lines. A. Effects of TNXB overexpression, 4 Gy radiation, and their combination on apoptosis rate in TE-1 and OE33 cells detected using flow cytometry. B. Effects of TNXB overexpression, 4 Gy radiation, and their combination on cell cycle distribution in TE-1 and OE33 cells detected using flow cytometry. **P < 0.01; ##P < 0.01.

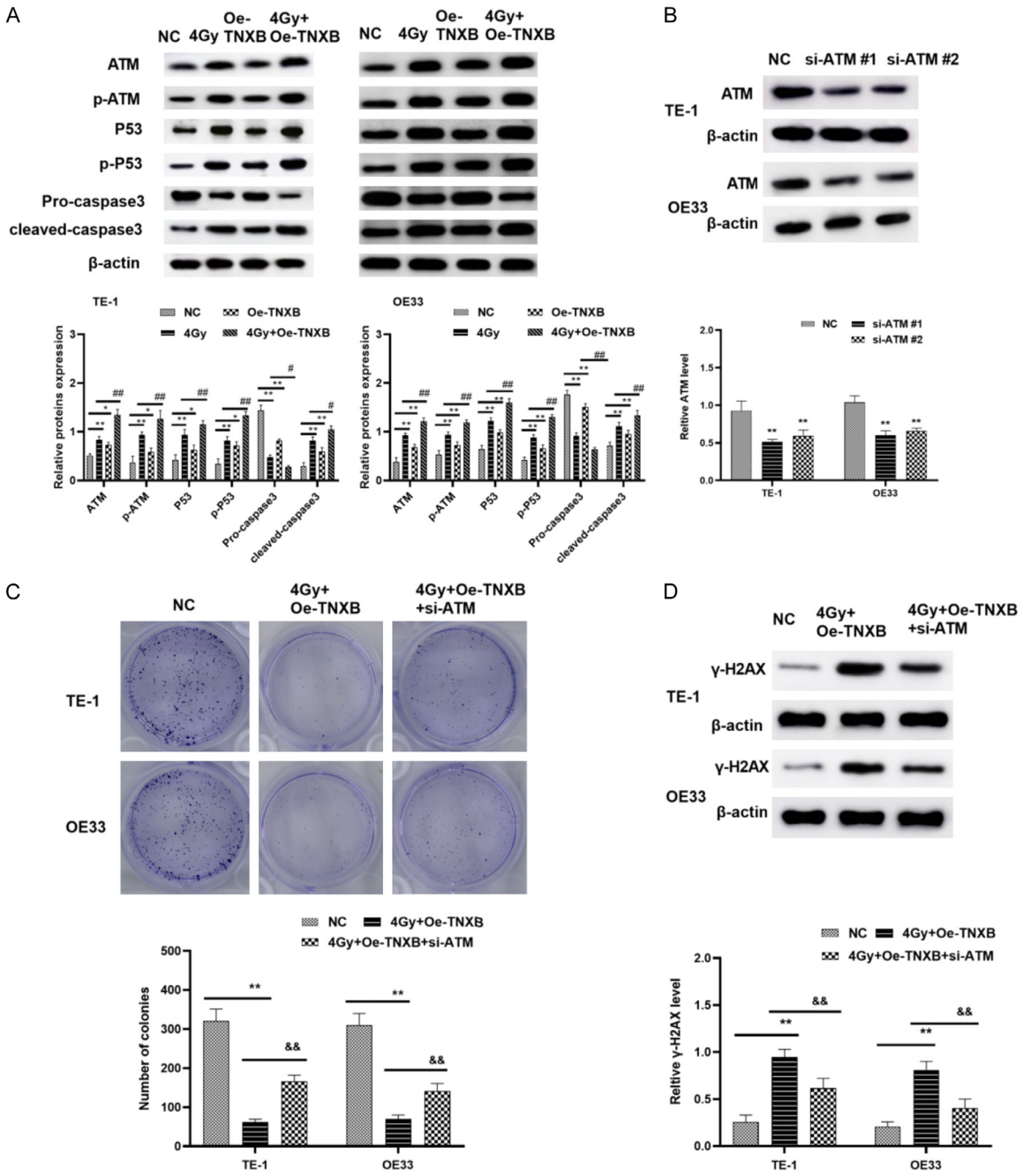

Figure 4. TNXB enhanced the radiotherapy-induced DNA damage through the ATM/P53 pathway. A. The expression of ATM/p53 pathway-associated proteins and apoptosis-related proteins in TE-1-Oe-TNXB and OE33-Oe-TNXB cells assessed using western blot assay. B. Transfection efficiency of si-ATM. C. Effects of ATM knockdown on colony formation of TE-1 and OE33 cells with TNXB overexpression following radiation. D. Expression of γ-H2AX in TE-1 and OE33 cells after ATM knockdown using western blot assay. *P < 0.05, **P < 0.01; #P < 0.05, ##P < 0.01; &&P < 0.01. ATM: Ataxia telangiectasia mutated.

Taken together, these results highlight TNXB as a critical mediator in both the prognosis and radiosensitivity of ESCA patients.

ATM is a 350 kD protein that plays a central role in coordinating the cellular response to DNA double-strand breaks, initiating a signaling cascade that leads to DNA repair, cell cycle checkpoints, or cell survival [22-24]. For example, ATM facilitates the G1/S cell cycle arrest by phosphorylating p53 at Ser15 [25]. The activation of ATM can also trigger senescence or

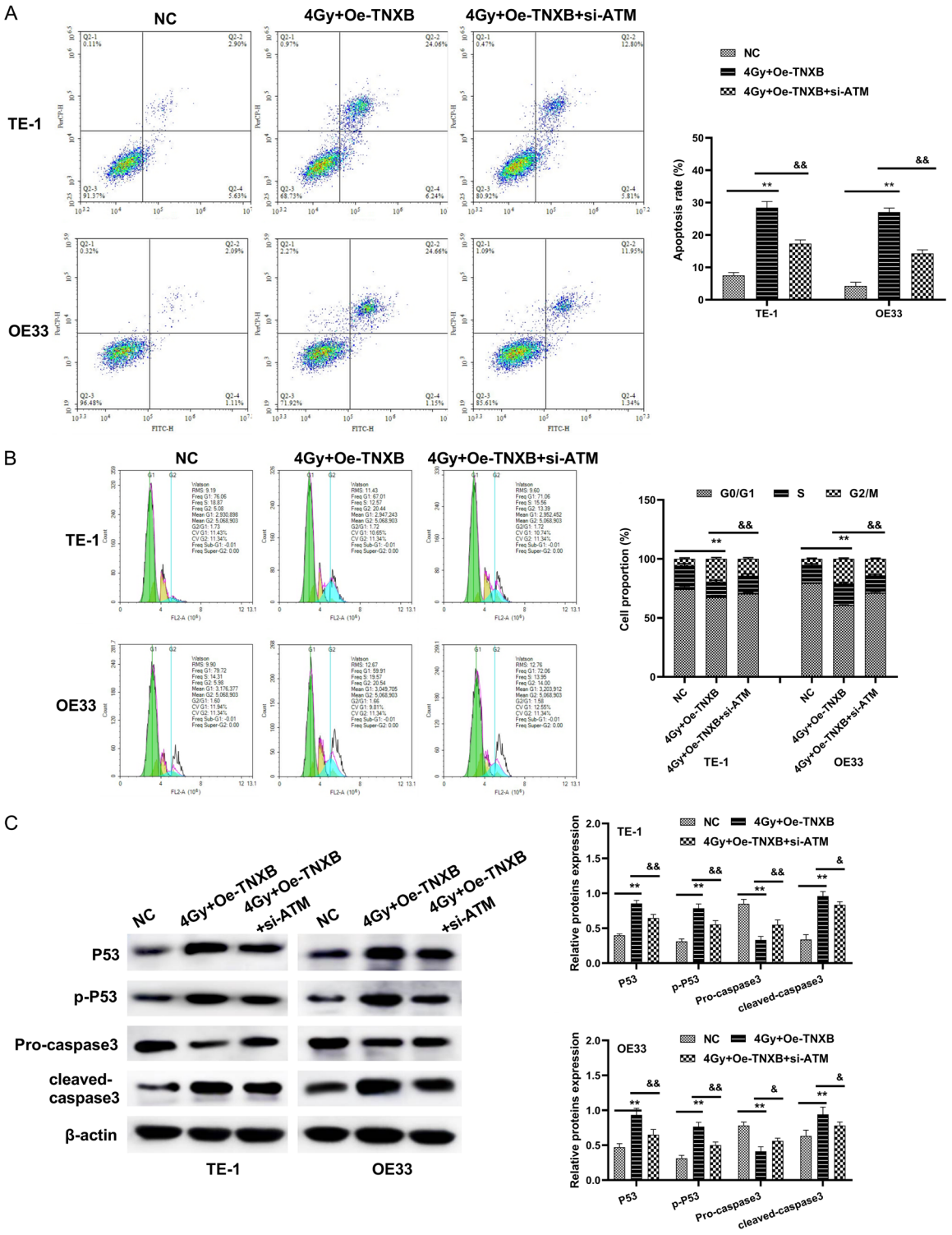

Figure 5. TNXB overexpression enhanced radiotherapy-induced apoptosis and G2/M arrest by the ATM/P53 pathway. A. Apoptosis rate in TE-1 and OE33 cells after ATM knockdown detected using flow cytometry. B. Cell cycle in TE-1 and OE33 cells after ATM knockdown detected using flow cytometry. C. Expression of p53 and apoptosis-related proteins in TE-1 and OE33 cells after ATM knockdown examined using western blot assay. **P < 0.01; &P < 0.05, &&P < 0.01.

apoptosis through phosphorylating p53, along with other targets involved in checkpoint activation in mammalian cells [26, 27]. The upregulation of ATM/ATR pathway proteins has been

shown to significantly inhibit the malignant growth of esophageal cancer cells [28]. Our work showed that depletion of ATM compromised the DNA damage response, cell cycle arrest, apoptosis and p53 phosphorylation induced by TNXB overexpression combined with irradiation *in vitro*.

Conclusion

TNXB functions by the ATM/p53 axis to induce tumor apoptosis and regulate the progression of ESCA after radiotherapy. These results suggest that targeting this pathway may be a promising therapeutic strategy for ESCA treatment.

Disclosure of conflict of interest

None.

Address correspondence to: Yipin Liu, Department of Gastroenterology, Binzhou Medical College Yantai Affiliated Hospital, No. 717 Jinbu Street, Yantai 264100, Shandong, China. E-mail: doctor_yhy@163.com

References

[1] Deng W, Yu R, Yang Z, Dong X and Wang W. Trends in conditional overall survival of esophageal cancer: a population-based study. Ann Transl Med 2021; 9: 102.

[2] Zhou J, Fang P, Li X, Luan S, Xiao X, Gu Y, Shang Q, Zhang H, Yang Y, Zeng X and Yuan Y. Prognostic value of geriatric nutritional risk index in esophageal carcinoma: a systematic review and meta-analysis. Front Nutr 2022; 9: 831283.

[3] Sardaro A, Ferrari C, Carbonara R, Altini C, Lavelli V and Rubini G. Synergism between immunotherapy and radiotherapy in esophageal cancer: an overview of current knowledge and future perspectives. Cancer Biother Radiopharm 2021; 36: 123-132.

[4] Yang X, Men Y, Wang J, Kang J, Sun X, Zhao M, Sun S, Yuan M, Bao Y, Ma Z, Wang G and Hui Z. Additional radiotherapy with or without chemotherapy following endoscopic resection for stage I esophageal carcinoma: a pilot study. Technol Cancer Res Treat 2021; 20: 15330338211048051.

[5] Yang X, Zhai Y, Bi N, Zhang T, Deng L, Wang W, Wang X, Chen D, Zhou Z, Wang L and Liang J. Radiotherapy combined with nimotuzumab for elderly esophageal cancer patients: a phase ii clinical trial. Chin J Cancer Res 2021; 33: 53-60.

[6] Wu J, Deng R, Ni T, Zhong Q, Tang F, Li Y and Zhang Y. Efficacy and safety of radiotherapy/chemoradiotherapy combined with immune checkpoint inhibitors for locally advanced stages of esophageal cancer: a systematic review and meta-analysis. Front Oncol 2022; 12: 887525.

[7] Kong Y, Su M, Fang J, Chen M, Zheng C, Jiang Y, Tao K, Wang C, Qiu G, Ji Y, Wang Y and Yang Y. Radiotherapy for patients with locally advanced esophageal squamous cell carcinoma receiving neoadjuvant immunotherapy combined with chemotherapy. Sci Rep 2024; 14: 16495.

[8] Okuda-Ashitaka E and Matsumoto KI. Tenascin-X as a causal gene for classical-like ehlers-danlos syndrome. Front Genet 2023; 14: 1107787.

[9] Marino R, Garrido NP, Ramirez P, Notaristefano G, Moresco A, Touzon MS, Vaiani E, Finkielstain G, Obregon MG, Balbi V, Soria I and Belgorosky A. Ehlers-danlos syndrome: molecular and clinical characterization of TNXA/TNXB chimeras in congenital adrenal hyperplasia. J Clin Endocrinol Metab 2021; 106: e2789-e2802.

[10] De Silva S, Alli-Shaik A and Gunaratne J. Machine learning-enhanced extraction of biomarkers for high-grade serous ovarian cancer from proteomics data. Sci Data 2024; 11: 685.

[11] Shi X, Sun Y, Shen C, Zhang Y, Shi R, Zhang F, Liao T, Lv G, Zhu Z, Jiao L, Li P, Xu T, Qu N, Huang N, Hu J, Zhang T, Gu Y, Qin G, Guan H, Pu W, Li Y, Geng X, Zhang Y, Chen T, Huang S, Zhang Z, Ge S, Wang W, Xu W, Yu P, Lu Z, Wang Y, Guo L, Wang Y, Guo T, Ji Q and Wei W. Integrated proteogenomic characterization of medullary thyroid carcinoma. Cell Discov 2022; 8: 120.

[12] Lu X, Fu Y, Gu L, Zhang Y, Liao AY, Wang T, Jia B, Zhou D and Liao L. Integrated proteome and phosphoproteome analysis of gastric adenocarcinoma reveals molecular signatures capable of stratifying patient outcome. Mol Oncol 2023; 17: 261-283.

[13] Song J and Yang H. Identifying new biomarkers and potential therapeutic targets for breast cancer through the integration of human plasma proteomics: a mendelian randomization study and colocalization analysis. Front Endocrinol (Lausanne) 2024; 15: 1449668.

[14] Yang N, Tian J, Wang X, Mei S, Zou D, Peng X, Zhu Y, Yang Y, Gong Y, Ke J, Zhong R, Chang J and Miao X. A functional variant in TNXB promoter associates with the risk of esophageal squamous-cell carcinoma. Mol Carcinog 2020; 59: 439-446.

[15] Zhang W, Zhu M, Xiang Y, Sun Y, Li S, Cai J and Zeng H. Current and future perspectives in un-

resectable locally advanced esophageal squamous cell cancer (Review). Oncol Rep 2024; 51: 65.
[16] Nakayama K, Seike M, Noro R, Takeuchi S, Matsuda K, Kunugi S, Kubota K and Gemma A. Tenascin XB is a novel diagnostic marker for malignant mesothelioma. Anticancer Res 2019; 39: 627-633.
[17] An L, Li M and Jia Q. Mechanisms of radiotherapy resistance and radiosensitization strategies for esophageal squamous cell carcinoma. Mol Cancer 2023; 22: 140.
[18] Liou Y, Lan TL and Lan CC. A meta-analysis and review of radiation dose escalation in definitive radiation therapy between squamous cell carcinoma and adenocarcinoma of esophageal cancer. Cancers (Basel) 2024; 16: 658.
[19] Liang G, Lv XF, Huang W, Jin YJ, Roquid KA, Kawase H and Offermanns S. Loss of smooth muscle tenascin-X inhibits vascular remodeling through increased TGF-beta signaling. Arterioscler Thromb Vasc Biol 2024; 44: 1748-1763.
[20] Liang G, Wang S, Shao J, Jin YJ, Xu L, Yan Y, Gunther S, Wang L and Offermanns S. Tenascin-X mediates flow-induced suppression of EndMT and atherosclerosis. Circ Res 2022; 130: 1647-1659.
[21] Matsumoto KI, Higuchi T, Umeki M, Ono M and Sakamoto S. Tenascin-X is increased with decreased expression of miR-378a-5p and miR-486-5p in mice fed a methionine-choline-deficient diet that induces hepatic fibrosis. Biomed Res 2024; 45: 67-76.
[22] Howes AC, Perisic O and Williams RL. Structural insights into the activation of ataxia-telangiectasia mutated by oxidative stress. Sci Adv 2023; 9: eadi8291.
[23] Mitiagin Y and Barzilai A. Ataxia-telangiectasia mutated plays an important role in cerebellar integrity and functionality. Neural Regen Res 2023; 18: 497-502.
[24] Hall MJ, Bernhisel R, Hughes E, Larson K, Rosenthal ET, Singh NA, Lancaster JM and Kurian AW. Germline pathogenic variants in the ataxia telangiectasia mutated (ATM) gene are associated with high and moderate risks for multiple cancers. Cancer Prev Res (Phila) 2021; 14: 433-440.
[25] Putti S, Giovinazzo A, Merolle M, Falchetti ML and Pellegrini M. ATM kinase dead: from ataxia telangiectasia syndrome to cancer. Cancers (Basel) 2021; 13: 5498.
[26] Gulliver C, Hoffmann R and Baillie GS. Ataxia-telangiectasia mutated and ataxia telangiectasia and Rad3-related kinases as therapeutic targets and stratification indicators for prostate cancer. Int J Biochem Cell Biol 2022; 147: 106230.
[27] Likhatcheva M, Gieling RG, Brown JAL, Demonacos C and Williams KJ. A novel mechanism of ataxia telangiectasia mutated mediated regulation of chromatin remodeling in hypoxic conditions. Front Cell Dev Biol 2021; 9: 720194.
[28] Wen J, Zhong X, Gao C, Yang M, Tang M, Yuan Z, Wang Q, Xu L, Ma Q, Guo X and Fang L. TPP1 inhibits DNA damage response and chemosensitivity in esophageal cancer. Crit Rev Eukaryot Gene Expr 2023; 33: 77-91.